VOL. 81, NO. 5 JOURNAL OF GEOPHYSICAL RESEARCH FEBRUARY 10, 1976

USGS Symposium on Long Valley, KGRA, California

Structure of Long Valley Caldera, California, From a Seismic Refraction Experiment

DAVID P. HILL

U.S. Geological Survey, Office of Earthquake Research, Menlo Park, California 94025

Two seismic refraction profiles crossing the Long Valley caldera in approximately east and north directions indicate that the crystalline basement with P wave velocities of 6.0 ± 0.4 km/s has been downdropped by 2.5–3 km across normal faults along the north and northwest sides of the caldera and 1–2 km along the south and east sides. Basement depths beneath the caldera floor range from between 3 and 4 km in the north and east sections to about 2 km in the central and south sections. Relief on the basement within the caldera suggests that the caldron block was partially disrupted during collapse, although a steplike offset in the eastern part of the basement may be due in part to precollapse displacement along the Hilton Creek fault. The distribution of P wave velocities in the caldera fill suggests that the Glass Mountain rhyolite and Bishop tuff have velocities of 4.0–4.4 km/s and the postcollapse rhyolite, rhyodacite, and basalt flows have velocities of 2.7–3.4 km/s. Domelike relief on the 4.0- to 4.4-km/s horizon indicates that postcollapse resurgence elevated the west central part of the caldera by about 1 km. Evidence for the roof of the magma chamber is contained in later arrivals tentatively identified as reflections from a low-velocity horizon at a depth of 7–8 km. Evidence for anomalous scattering or absorption properties associated with the region of shallow hydrothermal alteration and hot spring activity is contained in relative attenuation of high frequencies in a guided wave propagating through this region.

INTRODUCTION

Two seismic refraction profiles were shot across the Long Valley caldera during the last part of May 1973 as part of the U.S. Geological Survey's multidisciplinary investigation of this geothermal resource area. The primary objective of the seismic refraction experiment was to define the structure of the upper 5–10 km of the crust as a basis for a more complete understanding of the nature and development of what has been identified as the Long Valley resurgent caldron [*Smith and Bailey*, 1968; *Bailey et al.*, 1976]. Most of this paper is devoted to a description of the experiment and an interpretation of its results in terms of the subsurface structure of the caldera.

A secondary objective of the experiment involved an examination of the recorded wave forms for any evidence that may reflect the presence of a geothermal reservoir within the caldera or a possible magma chamber (either crystallized or molten) at depth. Little has been published on the application of active seismic methods to the study of geothermal systems [*Hayakawa*, 1970; *Hochstein and Hunt*, 1970], although recent developments in the recording and interpretation of seismic data offer considerable promise in this regard. The physical conditions thought to prevail in geothermal reservoirs, which include high temperatures, high porosity, fracture zones, etc. [*White*, 1973], suggest that the associated elastic properties should include relatively low seismic wave velocities, high attenuation (low Q), and local velocity heterogeneities resulting in anomalous wave scattering. *Hayakawa* [1970] cites evidence for some of these properties in data from the detailed seismic reflection survey in the Matsukawa geothermal field in Japan. This secondary objective met with at least partial success in that evidence in the seismograms was found for the roof of a magma chamber at a depth of 7–8 km as well as for near-surface effects of the hydrothermal area in the eastern section of Long Valley.

A number of geophysical studies in the Long Valley region are described in the literature. Most of this work involves seismic and gravity surveys by L. C. Pakiser and his colleagues as part of a continuing study of the tectonics and volcanism of the Owens Valley–Mono Lake region [*Pakiser et al.*, 1960; *Pakiser*, 1961; *Pakiser et al.*, 1964; *Pakiser*, 1968]. The regional crustal structure in the Long Valley–Mono Lake area is outlined by long-range seismic refraction profiles between Mono Lake and Lake Mead, Nevada [*Johnson*, 1965], and between China Lake and Mount Shasta [*Eaton*, 1966]. These studies indicate that the crust in the vicinity of Long Valley is characterized by (1) P wave velocities of 6.0–6.2 km/s near sea level (about 2 km below the surface) increasing to 6.4 km/s at depths of 25–30 km, (2) P wave velocities of 6.8–7.2 km/s in the lower 10–20 km of the crust, (3) a total crustal thickness of 40–50 km, and (4) upper mantle P wave (Pn) velocities of 7.8–7.9 km/s.

DESCRIPTION OF THE EXPERIMENT

The experiment consisted of two profiles crossing the caldera in roughly north and east directions. Locations of shot points and recording units along the two profiles, AA' and BB', are shown in Figure 1. Also shown are the caldera floor outline [*Bailey et al.*, 1976] and 10-mGal gravity contours adapted from *Pakiser et al.* [1964] and *Kane et al.* [1976]. Profile AA' extends in an ESE direction from the Deadman shot point at the northwest edge of the caldera to the Hammil shot point near the foot of the White Mountains. Profile BB' extends northward from the Convict shot point near the southern edge of the caldera to the Mono shot point 3 km south of Mono Lake. The profiles intersect near the center of the caldera in Little Antelope Valley; shot point Antelope is common to both profiles.

Data were obtained by 10 seismic refraction recording units held in fixed positions along a given profile as the individual shots along the profile were fired at half-hour intervals. Recording unit K at the Antelope shot point and units I and T at the east edge of the caldera were held in the same locations for all shots along both profiles. Recording units are the standard eight-channel U.S. Geological Survey seismic refraction trucks described by *Warrick et al.* [1961]. Each unit records the output of six vertical component seismometers in a linear array 2.5 km long together with WWV and WWVB time

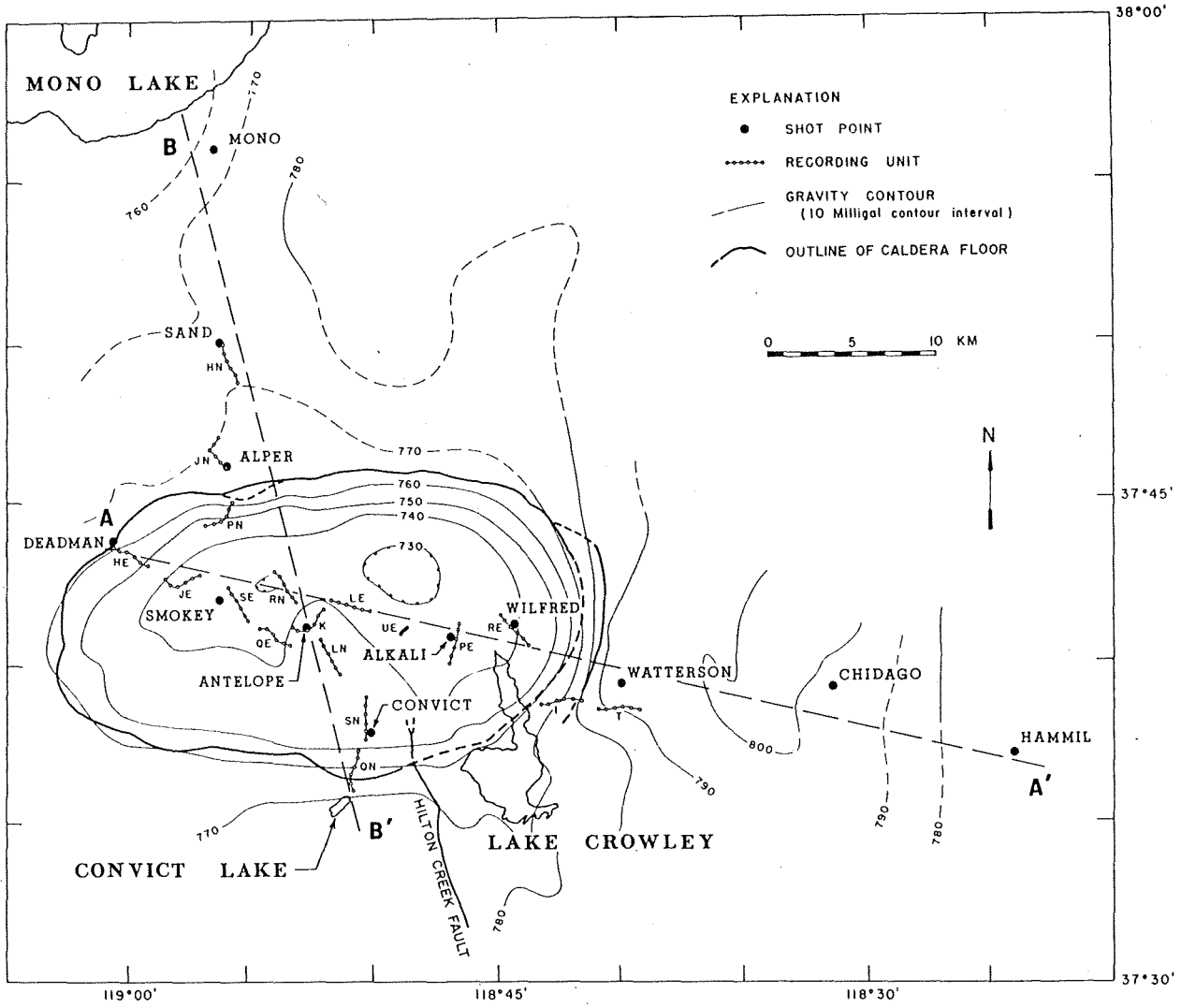

Fig. 1. Map showing locations of shot points and recording units with respect to the outline of the caldera floor and 10-mGal gravity contours. Caldera faults are closely associated with caldera floor outline [see *Bailey et al.*, 1976].

signals. Two horizontal component seismometers provide a three-component station at one of the verticals in the array. A Union Oil reflection crew operating in the area also recorded shots and provided analog copies of their records.

Shot times were determined to within ±0.01 s by recording the cap break and the output of an up-hole seismometer on two of the eight channels in an adjacent seismic refraction unit or on a special three-channel shot point recorder. Because of an equipment malfunction, however, the shot time at Smokey could only be determined to within 1 s. The shot at Hammil was weak and did not produce usable first arrivals on any of the recording units.

Travel times of first arrivals picked from analog records are plotted in Figures 2 and 3 for profiles AA′ and BB′. In addition, record sections for each shot point were generated by computer from digitized magnetic tapes. Examples of these record sections are shown in Figures 4, 5, and 6 for shot points Deadman, Alkali, and Mono, respectively. Locations, travel times, and a complete set of record sections are compiled in the report by *Hill and McHugh* [1975].

Interpretation

The geometry of the experiment is such that intersecting profiles, which individually provide two-dimensional information, are used to obtain a first approximation to the three-dimensional structure of the caldera. A basic assumption in the interpretation of the experiment is that the structure along each profile can be approximated by a series of homogeneous layers bounded by plane interfaces with dips parallel to the trend of the profile. The possibility of a change in dip of a given interface along the profile is included. Accordingly, the travel time data in Figures 2 and 3 were fitted with a series of straight line segments.

Figure 1 suggests the limitations inherent in the two-dimensional design and interpretation of this experiment. The distribution of shot points and recording units, which was constrained by topography, existing roads, and permitting considerations, deviates somewhat from forming linear profiles. This, coupled with the three-dimensional character of the structure implied by the gravity data, indicates that the nominally reversed travel time branches cannot necessarily be associated with reversed subsurface propagation paths and, further, that interfaces may have dips that deviate significantly from the vertical plane of the profile. The interpretation should be recognized for these limitations while at the same time it should be recognized that a more elaborate interpretation would require additional assumptions not justified by the available data.

By using the above assumption, models of the velocity structure along each profile were constructed by (1) applying standard equations for plane dipping layers [*Mota*, 1954] to the travel time branches between adjacent shot points to approximate the near-surface (upper 1–2 km) velocity structure, (2) establishing the *P* wave velocity for the basement refractor based on reversed travel time branches judged to have propagated along nearly reversed subsurface paths, and (3) using apparent velocities of travel time branches to establish dips on the basement surface together with graphical two-dimensional ray tracing to establish basement depths consistent with total travel times and the near-surface structure determined under (1).

The resulting velocity models along profiles AA′ and BB′ are shown in Figures 7 and 8, respectively.

Interfaces that can reasonably be interpreted as having subsurface reversal between adjacent shot points are indicated by heavy lines. Interfaces indicated by thin lines probably do not have subsurface reversal for reasons mentioned above. Extrapolated interfaces or interfaces based on secondary arrivals are indicated by dashed lines. The shot points are too widely separated to define continuous variations in the near-surface structure along the profiles, and details of how the near-surface structure between adjacent pairs of shot points should join remain unresolved.

The basement *P* wave velocity is shown as a uniform 6.0 km/s in the velocity models. This value is based on the reversed and overlapping travel time branches on profile BB′ north of the caldera between the Sand and Alper shot points, where the propagation paths probably approach true subsurface reversal. *Johnson* [1965] reports a similar value (6.15 km/s) at a depth of 1.6 km south of Mono Lake. Efforts to determine the basement *P* wave velocities within the caldera, assuming that the reversed and overlapping travel time curves on profile AA′ provide true subsurface reversal, lead to velocities of 5.6 km/s west of Antelope and 6.4 km/s east of Antelope. There is no a priori reason to reject lateral velocity variations of this size within the basement; indeed, L. C. Pakiser (personal communication, 1974) reports a *P* wave velocity of 5.35 km/s for the uppermost basement at depths of 1–2 km beneath Mono Lake only 25 km to the north. Because of the limitations mentioned above, however, it seems most reasonable to interpret the apparent lateral velocity variation in Long Valley as a ±0.4-km/s uncertainty in the 6.0-km/s value for the basement *P* wave velocity under the caldera. The associated uncertainty in depth to the basement is approximately ±3%, the lower velocity giving a greater depth.

Two solutions for the basement interface within the caldera are shown in Figures 7 and 8. They result from assuming a uniform basement velocity (6.0 km/s) and admitting that arrivals on the reversed travel time curves may have propagated along different paths within the basement. Solution A in Figure 7, for example, is based on the reversed travel time branches between Deadman and Antelope with apparent

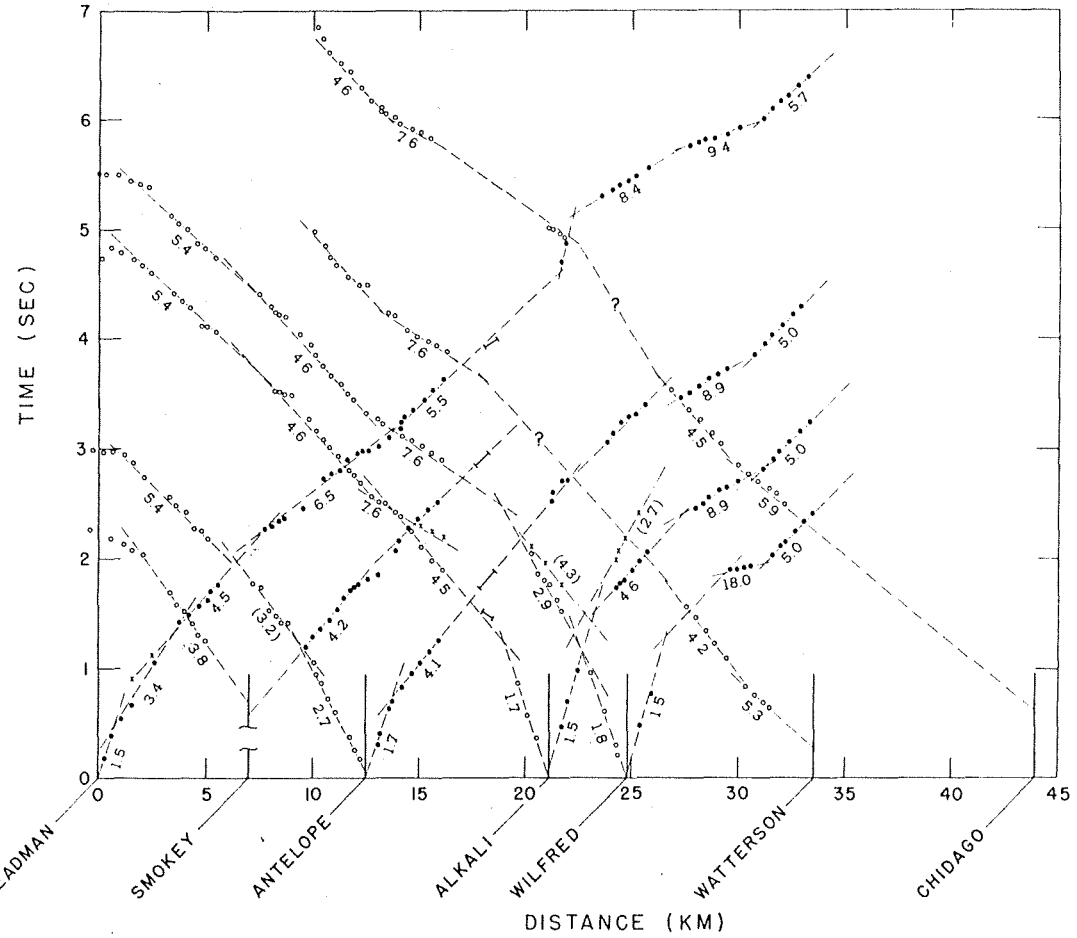

Fig. 2. Travel time curves along profile AA′. Circles and dots are first arrivals for waves propagating to the left and right, respectively. The crosses are later arrivals. The bars represent first arrivals recorded by the Union Oil reflection unit. Numbers are apparent velocities in kilometers per second. Parentheses indicate apparent velocities based on later arrivals or extrapolated travel time branches.

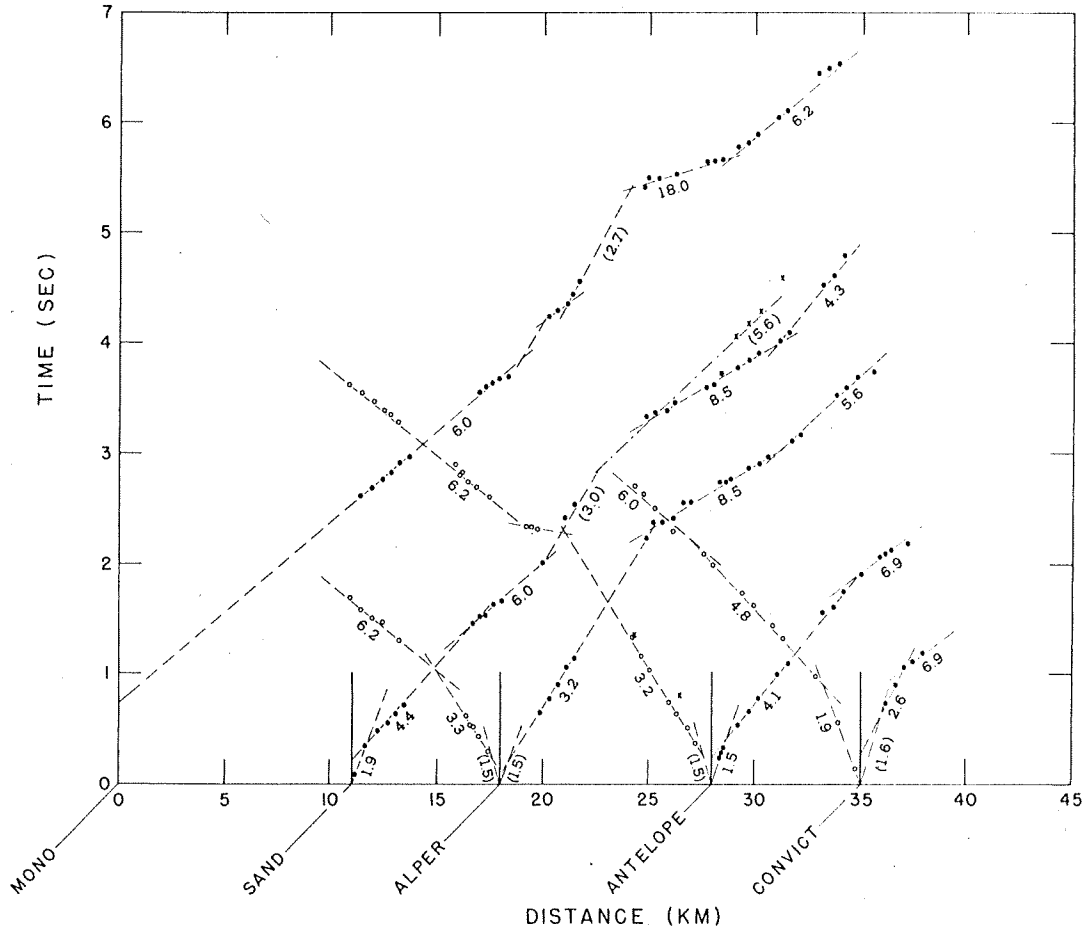

Fig. 3. Travel time curves along profile BB'. Symbols are the same as in Figure 2.

velocities of 6.5 and 5.4 km/s. The shot points and receivers lie nearly along a straight line in this interval (Figure 1). Solution B is based on overlapping travel time branches from Alkali and Wilfred with apparent velocities of 4.6 and 5.4 km/s. The distribution of shot points and recording units shown in Figure 1 suggests that these arrivals have propagated along paths that sample the basement somewhat closer to the gravity low on the north side of the caldera than those between Deadman and Antelope. The greater depth for solution B is generally consistent with the gravity gradient and the dip on the basement north of Antelope shown in profile BB' (Figure 8).

Factors such as the possible lateral propagation of waves in the three-dimensional caldera structure and subjective judgments in drawing travel time branches through the plotted points make a strictly quantitative assessment of the accuracy of the velocity models in Figures 7 and 8 difficult. My estimate

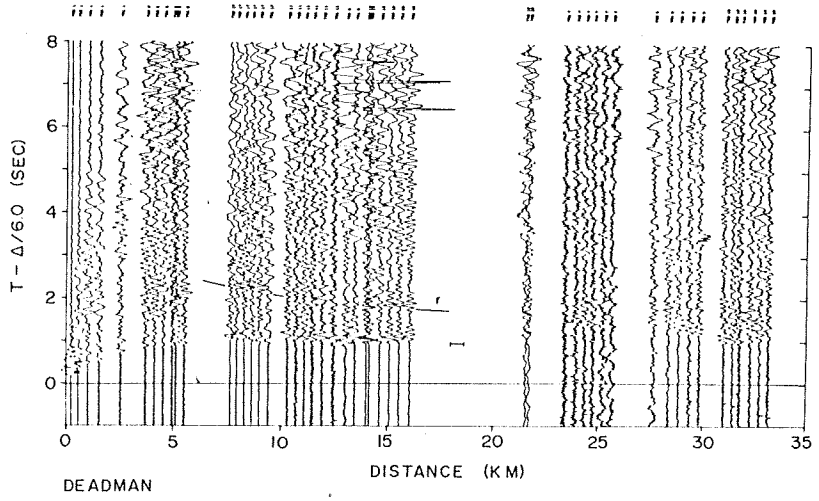

Fig. 4. Record section of seismograms recorded from the Deadman shot point. Amplitudes of each group of six traces from a given recording unit are normalized independently. Bar represents first arrivals recorded by Union Oil reflection unit; *r* indicates arrival, tentatively identified as a deep reflection.

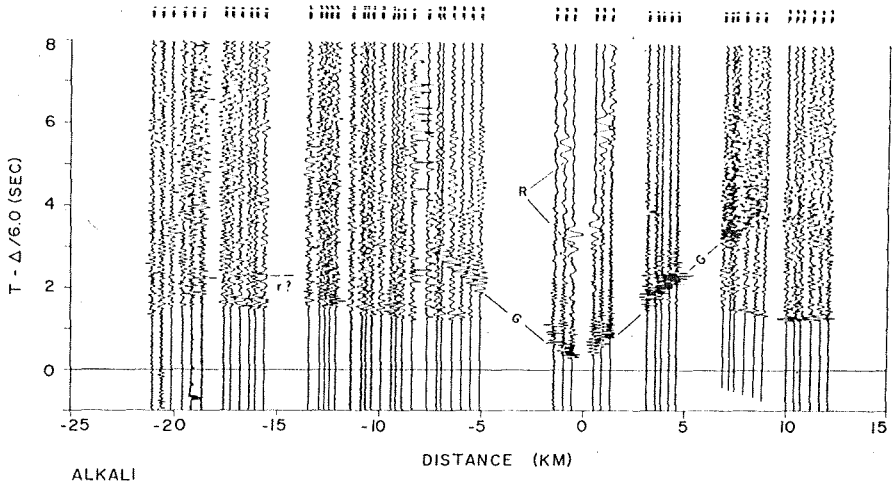

Fig. 5. Record section of seismograms recorded from the Alkali shot point. G indicates shallow guided wave group; R indicates surface wave.

of the overall accuracy of the models on the basis of experience with a number of different assumptions and solutions is that the *P* wave velocities of the various horizons are probably good to within ±10% and the depths of the interfaces are probably good to within ±20%.

Discussion

The velocity models in Figures 7 and 8 indicate that the upper surface of the basement within the caldera is at depths between 3 and 4 km beneath the north and east parts of the caldera and 1.5–2 km beneath the west central and southwest parts of the caldera. *P* wave velocities in the caldera fill overlying the basement increase from 1.5 km/s at the surface to 4.4 km/s at depth. Material with velocities from 4.0 to 4.4 km/s forms a continuous layer 1–2 km thick at the base of the caldera fill. Relief on the surface of this layer resembles a broad dome centered over the west part of the caldera. A layer with velocities between 2.7 and 3.4 km/s overlies the 4.0- to 4.4-km/s material and tends to be thickest over parts of the caldera where the basement is relatively deep. A surficial layer with velocities between 1.5 and 1.9 km/s and a thickness of 50–200 m overlies most of the west part of the caldera and is at least 0.5 km thick in the east part of the caldera.

P wave velocities and rock units. The subsurface distribution of major rock units illustrated in the east trending cross section through the caldera drawn by *Bailey et al.* [1976] on the basis of geologic field relations is remarkably similar to the distribution of seismic velocity horizons in profile AA′ (Figure 7). This similarity suggests the following association between seismic *P* wave velocities and rock units: 6.0 ± 0.4 km/s, Jurassic-Cretaceous granitic and Paleozoic-Mesozoic metamorphic basement rocks; 4.0–4.4 km/s, Bishop tuff and Glass Mountain rhyolite; 2.6–3.4 km/s, postcollapse rhyolites, rhyodacites, and basalts; 1.5–1.9 km/s, highly jointed near-surface volcanic rocks (weathered layer) in the west part of the caldera and alluvium and glacial, lake, and marsh deposits in the east.

Basement relief and gravity. Basement depths in the seismic velocity models along profiles AA′ and BB′ and the two-layer density model obtained by a three-dimensional interpretation of the gravity data by *Kane et al.* [1976] are also in reasonably close agreement. Evidently, the 0.45-g/cm³ density contrast used in the gravity interpretation is a good approximation of the average density contrast between the caldera fill and the basement.

The velocity models indicate a rather abrupt change in basement depth in the vicinity of the bounding caldera faults and steep gravity gradients. This relief on the basement is most clearly defined in profile BB′ just south of Alper where the depth to basement increases by 2.5–3 km in a distance of 5 km or less (see Figure 8). The solid line in this model represents the basement determined from Sand and Alper travel time curves, whereas the dashed line represents the basement determined from the Mono travel time curve (see Figure 3). High apparent velocities recorded near Deadman also indicate a steep dip on the basement at the west end of profile AA′, although the travel time data do not resolve the total relief on the basement. Granitic basement is exposed immediately west of the Deadman shot point, however, and if the 6.0-km/s horizon represents the top of the buried granitic basement, vertical relief across the caldera fault is 2.5–3 km here as well.

The moderate dip (about 15°) on the basement at the eastern edge of the caldera in the model for profile AA′ poses a problem in terms of the steep gravity gradient associated with the bounding faults. A profile across the gravity gradient, for example, can be fitted by a model with a 5 ± 2 km vertical step

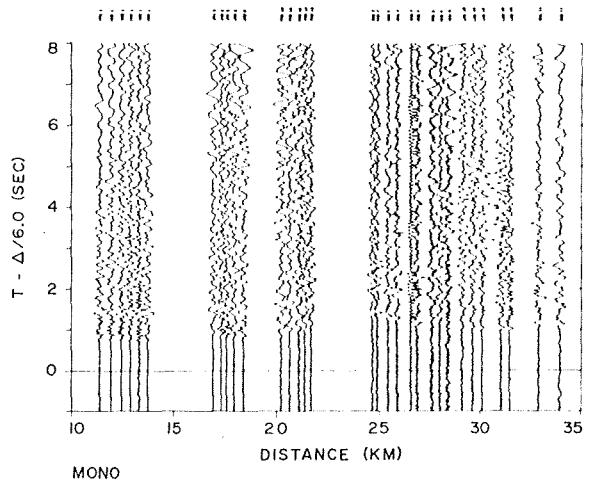

Fig. 6. Record section of seismograms recorded from the Mono shot point.

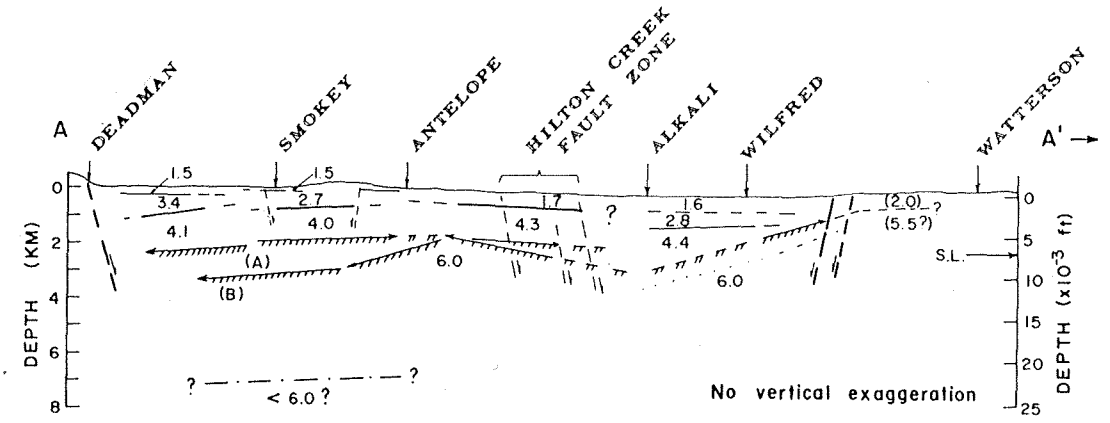

Fig. 7. Cross section showing *P* wave velocity structure under profile AA'. Numbers are *P* wave velocities in kilometers per second. Depths are with respect to average surface elevation (2.1 km); S.L. indicates sea level. Heavy lines indicate horizons with reversed subsurface coverage. Light lines indicate horizons with one-way subsurface coverage; arrows indicate propagation direction of subsurface waves along the horizon. Dashed lines indicate horizons based on later arrivals or extrapolated horizons. Basement horizon is indicated by hachures. Faults are indicated by steeply dipping dashed lines with arrows showing sense of displacement.

in the basement and a density contrast of 0.4 g/cm³ between the basement and the caldera fill [*Pakiser*, 1961; *Pakiser et al.*, 1964]. A more recent interpretation of the gravity field [*Kane et al.*, 1976] using a density contrast of 0.45 g/cm³ gives vertical relief in the basement across this zone of 3.3 km over a distance of about 2.5 km with an average dip of more than 50°. Resolution of this apparent discrepancy between the seismic and gravity interpretations may lie in the following explanations.

1. The locations of the recording units at the east end of the caldera depart from a simple profile normal to the gravity gradient, which tends to result in lower apparent velocities across the recording spreads than if the arrivals had propagated directly 'up dip.' The apparent continuity of travel time segments on the Deadman travel time curve recorded between Wilfred and Watterson, however, seems to preclude abrupt changes in basement depth in this interval.

2. The bulk density of the thick accumulation of low-velocity near-surface material in the east part of the caldera (Figure 2, also profile 6 in the work by *Pakiser et al.*, 1964] is not known but may be less than 2.0 g/cm³. Thus a significant part of the gravity low at the east end of the caldera could be attributed to these deposits. A similar explanation has resolved, in part at least, discrepancies between interpretations of the basement depth beneath Mono Lake [*Pakiser*, 1968; *Christensen et al.*, 1969; *Pakiser*, 1970].

Along similar lines, the 2.8- to 3.4-km/s layer may have a lower bulk density than might normally be associated with these *P* wave velocities. The rhyolites and rhyodacites presumed to form this horizon were erupted into a moat formed between the resurgent dome and the bounding caldera walls while the moat was occupied by the Pleistocene Long Valley Lake. Accordingly, there may be substantial thicknesses of lake and marsh deposits interbedded with the lava flows together with relatively coarse scree deposits from the steep, fault-controlled walls of the caldera (R. A. Bailey, personal communication, 1974). Such deposits would form low-velocity lenses within the 2.7- to 3.4-km/s layer that could not be detected by seismic refraction measurements on the scale of this experiment. If this is the case, then the average density of the caldera fill around the north and east sides of the caldera may be significantly lower than that in the west central part. The effect of correcting for such a lateral variation in the bulk density of the caldera fill would be to reduce the depths to the basement along the north and east margins of the caldera from those required in the single-density contrast gravity model.

Structural implications. Relief on the basement within the caldera can be attributed to (1) precollapse topography, (2) partial disruption or differential tilting during collapse of the caldera, (3) postcollapse resurgence, and (4) continuing tectonic displacement on throughgoing faults.

Bailey et al. [1976] suggest that the NNW trend of the gravity contours in the central part of the caldera [see *Kane et al.*, 1976] reflects precollapse displacement on the Hilton Creek fault that is preserved within the caldron block. The 0.5-s delay in the Deadman travel time curve in the vicinity of Alkali (Figure 2) indicates a vertical offset in the basement of about 1.5 km just west of Alkali that is consistent with displacement on the Hilton Creek fault (Figure 7). This offset, however, is somewhat east of the inferred location of the Hilton Creek fault zone and the maximum gravity gradient (Figure 1). How much of the vertical offset in the basement can be attributed to precollapse relief on the Hilton Creek fault is not clear. Some offset may have occurred during col-

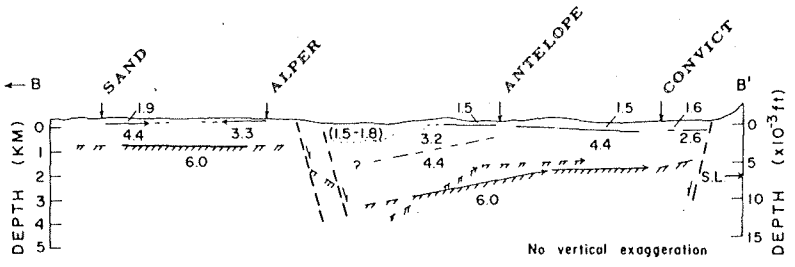

Fig. 8. Cross section showing *P* wave velocity structure under profile BB'. Symbols are the same as in Figure 7.

lapse as differential subsidence of the caldron block along this preexisting weak zone. Any offset due to postcaldera tectonic displacement on the fault should be reflected in the shallower horizons as well. Unfortunately, the solutions for the near-surface structure between Alkali and Antelope are ambiguous in this regard (see Figure 7).

The general configuration of the basement in Figures 7 and 8 suggests that the caldron block partially broke up during collapse. In particular, it appears that a north section of the block tilted to the north and the eastern section tilted to the west, some differential subsidence occurring across the preexisting Hilton Creek fault.

Relief on the top of the 4.0- to 4.4-km/s layer (the Bishop tuff?) describes a broad dome centered over the west part of the caldera. The geometry of this dome supports the pattern of resurgence associated with eruption of the central rhyolites inferred by *Bailey et al.* [1976] from dips on central rhyolite tuffs and elevations of fossil shore lines of Pleistocene Long Valley Lake. The velocity models (Figures 7 and 8) suggest that maximum uplift in the center of the resurgent dome is between ½ and 1 km. A smooth connection of the 4.3- and 4.4-km/s layers on either side of Alkali (see Figure 7) would be consistent with this resurgence and in turn would eliminate the necessity for significant postcollapse tectonic displacement on the Hilton Creek fault within the caldera.

Possible evidence for a magma chamber. A set of later arrivals, following the first arrivals by 1.2–0.7 s is clearly evident on the Deadman record section (Figure 4) over the distance interval 7–16 km. These arrivals have a somewhat higher apparent velocity than the first arrivals; they also appear to be 180° out of phase with respect to the first arrivals. The latter can be demonstrated by tracing the first arrivals in the distance range 15–16 km and matching the later arrivals with the tracing inverted. Evidence for a similar, but weaker, set of arrivals can be seen on the Alkali record section in the distance range −12 to −17 km. The least complicated interpretation of these arrivals is that they have been reflected from a horizon within the basement at a depth of 7–8 km (Figure 7) across which the velocity decreases with depth.

Such a reflecting horizon is a likely candidate for association with the roof of the magma chamber that fed the eruption of the Bishop tuff and subsequent rhyolite eruptions. *Bailey et al.* [1976] infer from the geometry of the resurgent dome that the roof of the magma chamber at the time of resurgence was at a maximum depth of 5–7 km. *Steeples and Iyer* [1976] find evidence in teleseismic *P* wave delays for a volume beneath the caldera extending from depths of approximately 5–25 km in which the average *P* wave velocity is 15% lower than the surrounding crust. The character of the later arrivals is consistent with either a reflection from a solid-melt interface or from a solid-solid interface, the deeper solid having a lower *P* wave velocity (i.e., a crystallized residual melt fraction?).

The secondary arrivals identified as deep reflections may, of course, have other explanations. They could, for example, be lateral reflections or refractions from a steeply dipping boundary out of the plane of the profile. The most likely alternative is that they are multiple refractions from the basement involving one reflection from the earth's surface. Such arrivals would also have a 180° phase shift with respect to the first arrivals, but they should also have the same apparent velocity as the first arrivals. The higher apparent velocity of the later arrivals in the record section thus supports their identification as deep reflections.

Evidence for the hydrothermal system. The shot at Alkali generated a strong set of secondary arrivals that were recorded to a distance of 7–9 km on either side of the shot point (G in Figure 5). These arrivals have an apparent velocity of 1.9 km/s and form essentially continuous travel time curves with the first arrivals, which have apparent velocities of 1.5 and 1.7 km/s (Figure 2). The large amplitudes and extended coda of these arrivals suggest that they are generated by a series of supercritical reflected and refracted waves propagating between the base of the 0.5-km-thick, 1.5- to 1.9-km/s layer and the free surface. There is a close analogy between these arrivals and the $\bar{P}$ phase in crustal seismology.

One of the more striking aspects of these secondary arrivals is the pronounced difference in frequency content between wave groups on either side of the shot point: the waves propagating to the west are notably deficient in high-frequency energy with respect to those propagating to the east. The amplitude spectra of the wave groups from seismograms recorded at approximately 5 km on either side of the shot point plotted in Figure 9 emphasize this difference. Note in particular the rapid falloff of spectral amplitudes above about 8 Hz in the wave group that propagated to the west. The spectrum of the wave group that propagated to the east peaks at about 15 Hz. (The computed spectral amplitudes are not reliable for frequencies below 1–2 Hz; thus the apparent difference in spectral amplitudes between the two wave groups below about 3 Hz is of questionable significance.) The waves

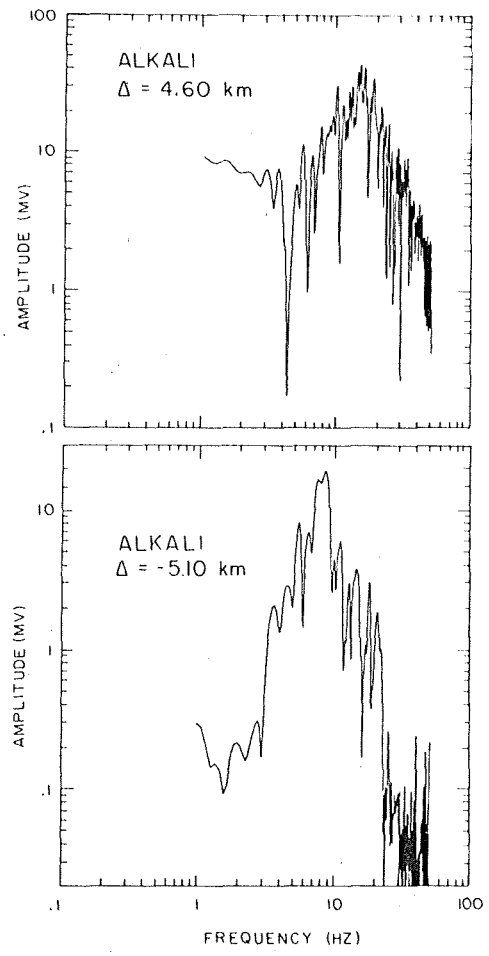

Fig. 9. Amplitude spectra of 1.9-km/s wave group from seismograms recorded 4.60 km east of Alkali (upper) and 5.10 km west of Alkali (lower) (see Figure 5). Ordinate is output of seismometer in millivolts. Amplitudes are not reliable for frequencies below about 2 Hz.

on the west side of the shot point have propagated across the main zone of shallow hydrothermal alteration and current hot spring activity in Long Valley (see Figure 5 in the work by *Bailey et al.* [1976]). The observed differences in the wave groups are very likely due to shallow scattering or attenuation properties of the hydrothermal area, the location of which is apparently controlled by north to northwest trending faults in the Hilton Creek fault zone [*Rinehart and Ross,* 1964]. Heterogeneities such as the vertical honeycomb or pipelike structures that are widespread in the hydrothermal area [*Bailey et al.,* 1976] would certainly provide a scattering mechanism, as would the fault zone itself. Although these data do not provide obvious clues to the deeper, poorly understood parts of the Long Valley hydrothermal system, it is encouraging to find what appears to be clear modification of the wave forms by shallow properties of the system.

As an aside, it is of interest to note the surface wave pulse recorded on the first two seismometers on either side of the Alkali shot point (R in Figure 5). The group velocity of this pulse is approximately 0.16 km/s, and its dominant period is about 0.3 s. This is virtually the same as the dominant group velocity and period associated with the microseismic noise in the east part of Long Valley described by *Iyer and Hitchcock* [1976] in their investigation of geothermal noise. Published dispersion curves from surface wave studies of shallow and sedimentary structures [*Dobrin et al.,* 1951] suggest that these waves may be an Airy phase of fundamental mode Rayleigh waves propagating in the lake and marsh deposits (the 0.5-km-thick layer with P wave velocities of 1.5–1.9 km/s).

CONCLUSIONS

The seismic refraction data obtained in this experiment provide a good first approximation to the P wave velocity structure of the upper 5–6 km of the crust beneath the Long Valley caldera. Tentative identification of horizons in the P wave velocity model with major rock units recognized in the caldera leads to the following conclusions.

1. The Sierran basement rocks in the caldron block (Cretaceous granitic rocks and Paleozoic to Mesozoic metamorphic rocks with P wave velocities of 6.0 ± 0.4 km/s) have been downdropped 2.5–3 km along normal faults bounding the north and northwest sides of the caldera. Displacement of the basement along normal faults bounding the south and east sides of the caldera is not well defined by the seismic data but generally appears to be between 1 and 2 km. There is an apparent discrepancy between the steep gravity gradients and the relatively small displacements and shallow dips of the basement suggested by the seismic data at the east margin of the caldera that may be explained in part by relatively thick accumulations of low-density sediments in that area.

2. Relief on the basement within the caldera suggests that the caldron block was partially disrupted during the collapse accompanying eruption of the Bishop tuff with the north part of the block tilting to the north and the east part of the block tilting to the west. A steplike displacement in the basement associated with the northward extension of the Hilton Creek fault into the caldera may be partly due to precollapse displacement along the Hilton Creek fault and partly due to differential settling of the basement during collapse along the preexisting weak zone formed by the fault.

3. The top of the 4.0- to 4.4-km/s layer, which overlies the basement and is tentatively identified with the Bishop tuff and Glass Mountain rhyolite, has a broad domelike structure centered over the western part of the caldera. This structure reflects postcollapse resurgence accompanying eruption of the central rhyolites. Maximum relief on the dome is from ½ to 1 km. Similar doming tends to be reflected in the basement as well, although it is partly obscured by relief on the basement.

4. The layer with P wave velocities of 2.7–3.4 km/s that overlies the 4.0- to 4.4-km/s layer is thickest in the moat between the resurgent dome and the caldera walls. This layer corresponds to the postcollapse rhyolites, rhyodacites, and basalt flows described by *Bailey et al.* [1976]. Substantial lake and marsh deposits from Pleistocene Long Valley Lake as well as clastic alluvial and glacial deposits are probably interbedded with these lava flows. Such interbedded deposits would result in a relatively low bulk density for this layer and may contribute significantly to the pronounced gravity lows observed along the north and northeast parts of the caldera. The permeability associated with substantial clastic deposits interbedded with the lava flows would also make the thicker sections of the 3.3- to 3.4-km/s layer filling the moat along the north and northwest margins of the caldera potentially favorable reservoirs for geothermal fluids.

5. The generally favorable agreement for basement depth in the caldera between the seismic refraction and three-dimensional gravity interpretations suggests that 0.45 g/cm^3 is a good approximation to the average density contrast between the caldera fill and the basement. The possibility that the 2.7- to 3.4-km/s material filling the moat may have a lower than average bulk density, however, suggests that the gravity lows may not require the deep depressions in the basement along the northern and northeast parts of the caldera shown in the single-density contrast model [*Kane et al.,* 1976]. The effect of the relatively thick, low-velocity (and presumably low-density) lake and marsh deposits in the east part of the caldera will also tend to reduce the depth to the basement shown in the gravity model.

6. Clear secondary arrivals on the Deadman record section are tentatively identified as a reflection from a low-velocity horizon at a depth of 7–8 km beneath the western section of the caldera. This horizon may be associated with the roof of the magma chamber beneath the caldera in the form of a trapped melt or a crystallized lens of low-velocity residual material.

7. And finally, the relative deficiency of high-frequency energy observed in a group of shallow guided waves provides evidence for anomalous scattering or attenuation associated with the region of hydrothermal alteration and hot spring activity in the eastern part of the caldera.

Acknowledgments. I am grateful to Wayne Jackson and Gene Taylor for their invaluable help with the logistics of the field program and to Stuart McHugh for his careful handling of the initial data reduction. I am particularly grateful to L. C. Pakiser for his encouragement and interest in all phases of the experiment. L. C. Pakiser and Roy A. Bailey critically reviewed the manuscript and suggested a number of improvements.

REFERENCES

Bailey, R. A., G. B. Dalrymple, and M. A. Lanphere, Volcanism, structure and geochronology of Long Valley Caldera, Mono County, California, *J. Geophys. Res., 81,* this issue, 1976.

Christensen, M. N., C. M. Gilbert, K. R. Lajoie, and Y. Al-Rawi, Geological-geophysical interpretation of Mono Basin, California-Nevada, *J. Geophys. Res., 74,* 5221–5239, 1969.

Dobrin, M. B., R. F. Simon, and P. L. Lawrence, Rayleigh waves from small explosions, *Eos Trans. AGU, 32,* 822–832, 1951.

Eaton, J. P., Crustal structure in northern and central California from

seismic evidence, Geology of Northern California, edited by E. H. Bailey, *Calif. Div. Mines Geol. Bull., 190,* 419–426, 1966.
Hayakawa, M., The study of underground structure and geophysical state in geothermal areas by seismic exploration, *Geothermics, Spec. Issue 2, 2,* 347–357, 1970.
Hill, D. P., and S. McHugh, A compilation of data from the 1963 Long Valley seismic-refraction experiment, open file report, U.S. Geol. Surv., Menlo Park, Calif., 1975.
Hochstein, M. P., and T. M. Hunt, Seismic gravity and magnetic studies, Broadlands geothermal field, New Zealand, *Geothermics, Spec. Issue 2, 2,* 333–346, 1970.
Iyer, H. M., and T. Hitchcock, Seismic noise survey in Long Valley, California, *J. Geophys. Res., 81,* this issue, 1976.
Johnson, L. R., Crustal structure between Lake Mead, Nevada, and Mono Lake, California, *J. Geophys. Res., 70,* 2863–2872, 1965.
Kane, M. F., D. R. Mabey, and R. L. Brace, A gravity and magnetic investigation of Long Valley caldera, Mono County California, *J. Geophys. Res., 81,* this issue, 1976
Mota, L., Determination of dip and depths of geological layers by the seismic-refraction method, *Geophysics, 19,* 242–254, 1954.
Pakiser, L. C., Gravity, volcanism, and crustal deformation in Long Valley, California, *U.S. Geol. Surv. Prof. Pap. 424-B,* B250–B253, 1961.
Pakiser, L. C., Seismic evidence for the thickness of Cenozoic deposits in Mono Basin, California, *Geol. Soc. Amer. Bull., 79,* 1833–1838, 1968.
Pakiser, L. C., Structure of Mono Basin, California, *J. Geophys. Res., 75,* 4077–4080, 1970.
Pakiser, L. C., F. Press, and M. F. Kane, Geophysical investigation of Mono Basin, California, *Geol. Soc. Amer. Bull., 71,* 415–447, 1960.
Pakiser, L. C., M. F. Kane, and W. H. Jackson, Structural geology and volcanism of the Owens Valley region, California—A geophysical study, *U.S. Geol. Surv. Prof. Pap. 438,* 68 pp., 1964.
Rinehart, C. D., and D. C. Ross, Geology and mineral deposits of the Mount Morrison quadrangle, Sierra Nevada, California, *U.S. Geol. Surv. Prof. Pap. 385,* 106 pp., 1964.
Smith, R. L., and R. A. Bailey, Resurgent cauldrons, *Geol. Soc. Amer. Mem., 116,* 613–662, 1968.
Steeples, D. W., and H. M. Iyer, Low-velocity zone under Long Valley as determined from teleseismic events, *J. Geophys. Res., 81,* this issue, 1976.
Warrick, R. E., D. B. Hoover, W. H. Jackson, L. C. Pakiser, and J. C. Roller, The specification and testing of a seismic-refraction system for crustal studies, *Geophysics, 26,* 820–824, 1961.
White, D. E., Characteristics of geothermal resources in *Geothermal Energy,* edited by P. Kruger and G. Otte, pp. 69–94, Stanford University Press, Palo Alto, 1973.

(Received January 29, 1975;
revised July 22, 1975;
accepted July 24, 1975.)